REPORT DOCUMENTATION PAGE

AFRL-SR-AR-TR-04-

0091

1. AGENCY USE ONLY *(Leave blank)*	2. REPORT DATE	3. REPORT TY
	29 JAN 04	FINAL REPORT 1 APR 01 TO 14 JUL 03

4. TITLE AND SUBTITLE
NEXT GENERATION AEROSPACE COMPOSITES THROUGH NANOTECHNOLOGY

5. FUNDING NUMBERS
F49620-01-1-0299

6. AUTHOR(S)
PROF. D. RAGHAVAN

7. PERFORMING ORGANIZATION NAME(S) AND ADDRESS(ES)
HOWARD UNIVERSITY
DEPT OF CHEMISTRY
525 COLLEGE STREET, ROOM 120
WASHINGTON, DC 20059

8. PERFORMING ORGANIZATION REPORT NUMBER

9. SPONSORING/MONITORING AGENCY NAME(S) AND ADDRESS(ES)
AFOSR/NL
4015 WILSON BLVD., ROOM 713
ARLINGTON, VA 22203-1954

10. SPONSORING/MONITORING AGENCY REPORT NUMBER

11. SUPPLEMENTARY NOTES

12a. DISTRIBUTION AVAILABILITY STATEMENT
APPROVE FOR PUBLIC RELEASE: DISTRIBUTION UNLIMITED

12b. DISTRIBUTION CODE

13. ABSTRACT *(Maximum 200 words)*

In recent years, the area of nanocomposites has received considerable attention with the expectation that nanotechnology can leas to lighter, better materials for engineering applications. For example, the attractiveness of polymer-clay nanocomposites resides in the potential of adding infinitesimally small clay platelets, to improve mechanical, thermal, barrier, and flame-retardant properties without increasing the specific gravity or reducing the transparency of the nanocomposite relative to the base material. One of the major roadblocks in the wider use of nanoclay platelets in thermoset and thermoplastic polymeric materials has been the poor dispersion of polar clay into a non-polar polymer matrix. It is believed that consistent improvements in strength and modulus of clay loaded polymeric system can be achieved by minimizing clay aggregation, promoting the formation of chemical bonds between polymer and clay and achieving exfoliation of clay. The other major problem that the nanocomposite community faces is the reduction in fracture toughness and failure strain of the nanocomposites due to the addition of clay.

14. SUBJECT TERMS

16. PRICE CODE

17. SECURITY CLASSIFICATION OF REPORT	18. SECURITY CLASSIFICATION OF THIS PAGE	19. SECURITY CLASSIFICATION OF ABSTRACT	20. LIMITATION OF ABSTRACT

Next Generation Aerospace Composites Through Nanotechnology

D. Raghavan

Professor

Department of Chemistry

Howard University

Washington, DC 20059.

Final Report :

Dr. Charles Lee (Program Manager)

AFOSR/NL

4015 Wilson Blvd., Room 713

Arlington, VA 22203-1977

OBJECTIVES :

The primary objective of this study is to develop a methodology for exfoliating clay platelets in polymeric resin and maintain high level of dispersion during the curing reaction. The other objective of this study was to improve the toughness of nanocomposite.

PROBLEM STATEMENT:

In recent years, the area of nanocomposites has received considerable attention with the expectation that nanotechnology can lead to lighter, better materials for engineering applications. For example, the attractiveness of polymer-clay nanocomposites resides in the potential of adding infinitesimally small clay platelets, to improve mechanical, thermal, barrier, and flame-retardant properties without increasing the specific gravity or reducing the transparency of the nanocomposite relative to the base material. One of the major roadblocks in the wider use of nanoclay platelets in thermoset and thermoplastic polymeric materials has been the poor dispersion of polar clay into a non-polar polymer matrix. It is believed that consistent improvements in strength and modulus of clay loaded polymeric system can be achieved by minimizing clay aggregation, promoting the formation of chemical bonds between polymer and clay and achieving exfoliation of clay. The other major problem that the nanocomposite community faces is the reduction in fracture toughness and failure strain of the nanocomposites due to the addition of clay.

BACKGROUND

Clay Exfoliation in Thermoset Matrix

Nanocomposite materials garner most of their material improvements from molecular interactions of clay and polymeric resin. Of particular interest in this study is the interaction of nanoclay platelet with epoxy and vinyl ester resin. The successful use of nanoclay reinforcement technology to improve the performance of polymeric resin would depend on the compatability of nanoclay platelets with polymer matrix.

An approach to improve the compatibility between the clay and polymer is to perform ion exchange reaction of Na^{+}, Ca^{+2}, or K^{+} with a *long chain cation* so as to increase the organophilicity of the clay surface layer and provide sufficient layer separation for few polymer chains to infilterate. Until now, most of the

intercalation/exfoliation studies on nanocomposites have been carried out by exchanging the cations on clay with long chain length non-bonding ammonium salt. Another approach commonly used to provide clay platelet separation is to suspend the clay particles in a polar solvent/monomer medium so as to promote polymer penetration between clay galleries. The criteria for monomer selection are based on its miscibility with the polymer and its ability to swell the organically modified clay. Both these approaches are attractive, and they provide a framework to explore the role of reactive onium salt in clay platelet separation of polymer nanocomposite. Very few studies have dealt with the role of a reactive onium salt that has structural similarity or reactivity towards polymer matrix in formulating polymer nanocomposite. The initial work by Toyota researchers in formulating nylon nanocomposites was based on functionalizing montmorillonite clay with 12-aminolauric acid. This work clearly demonstrated the desirability of using onium salts having a functional group for clay platelet separation. Although the role of reactive salts in nanocomposites is implied from this work, specific examples related to montmorillonite clay functionalized with vinyl-terminated ammonium salts for vinyl ester system and clay functionalized with hydroxyl/epoxy group for epoxy resin system are not available in the open literature. The use of functionalized clay to improve clay dispersion in thermoset resin and improve the mechanical properties of nanocomposite is an interesting concept not fully explored.

Toughening of Nanocomposite

The dispersion of nanoclay platelets in polymeric resin is known to reduce the failure strain of the nanocomposites. Little is known about how to improve the failure strain and toughness of nanocomposites. Indeed, this problem has been addressed by use of conventional rubber toughening technology in brittle epoxies. We showed that epoxy resin toughness can be greatly improved by the addition of ~15 phr (parts per hundred of epoxy resin) of acrylic rubber dispersants (0.25 μm) to epoxy resin without sacrificing the Tg of resin. The retention of Tg of cured resin after rubber particle dispersion indicates that the acrylic rubber is generally well phase separated. The retention of Tg of cured resin in rubber particle dispersed epoxy is important given that improvement in toughness of resin by adding rubber dispersants is often obtained at the expense of Tg of resin.

The successful use of rubber dispersion technology to improve the failure strain and toughness of clay filled epoxy resin would represent an important development in the formulation of matrix material for advanced structural application, whose desired failure behavior is ductile. Therefore, the other objective of this study is to demonstrate that dispersion of clay platelets and rubber dispersants in epoxy leads to overall improvement of strength, modulus, and break strain of the rubber dispersed epoxy nanocomposite.

For achieving dispersion of clay in resin, the emphasis is placed on the synthesis of reactive onium salt and the role of reactive onium ion modified clay over non-reactive onium ion modified clay in the presence of diluent in promoting *clay platelet separation* of clay polymer nanocomposite. Two types of reactive onium salt were synthesized of different chain length. While reactive long chain length (C19) and medium chain length (C11) onium salts were synthesized in the laboratory, commercially available non-reactive long chain length (C18) and medium chain length (C11) onium salts were used for the study without further purification. In this research, the sodium ions in the clay are exchanged with onium ions (a mixture of reactive and non-reactive onium salt). The hydroxyl groups of reactive onium salts are expected to facilitate the miscibility of DGEBA monomer with clay platelets, while the olefinic groups of reactive onium salts are expected to facilitate the miscibility of vinylic resin with clay platelets. The morphology of clay nanocomposite and rubber filled nanocomposites was characterized by X-ray diffraction (XRD), transmission electron microscopy (TEM), and the mechanical properties of clay filled and rubber filled nanocomposite was obtained by performing tensile test characterization.

EXPERIMENTAL

A. Formulation of Nanocomposite

A.1 Synthesis of reactive long chain length onium salt

The reactive onium salt (hydroxyl functionalized C19 amine hydrochloride) was synthesized from renewable resource (vernonia oil) through series of synthetic conversion. Figure 1 is a schematic representation of the conversion of vernanol (alcohol synthesized from vernonia oil) to hydroxyl functionalized C19 amine hydrochloride. The oil was initially transesterified under basic medium and the intermediate was reduced using lithium aluminum hydride in hexane medium to obtain cis12, 13-epoxy-cis-9-

nonadecenol (vernanol) as primary product. Vernanol was then converted into vernanyl mesylate, followed by reaction with potassium cyanide to obtain 13, 14-epoxy-cis-10-nonadecenitrile (C-19 nitrile). The C-19 nitrile was reduced with Lithium Aluminum Hydride in ether medium and then converted with HCl acid into 13 (14) Hydroxyl cis – 10-nonadecenyl amine hydrochloride (C-19 amine hydrochloride). The proton NMR (Figure 2) of the reactive onium salt showed an intense singlet peak corresponding to a chemical shift at 8.2 δ, characteristic of primary amine hydrochloride in the final compound. The C13 NMR spectrum (Figure 3) showed characteristic peaks for secondary alcohol groups at 62 δ and 70 δ, which suggests that the epoxy ring has opened during LAH reduction of nitrile compound. Figure 4 gives the MALDI-TOF mass spectra for C-19 amine hydrochloride. The diagnostic ions that were observed in the MALDI spectral data of the primary ammonium ion correspond to M^+ and $M+1^+$ peaks at m/z 298.5 and 299.5 amu respectively. Details about the synthesis and characterization of onium salt can be found elsewhere [1].

A.2 Synthesis of reactive medium chain length onium salt

Figure 5 provides the reaction sequence used in the synthesis of ω–undecylenyl amine hydrochloride (reactive onium salt) from undecylenol. In this multi-step synthetic strategy for forming reactive medium chain length onium salt, ω–undecylenol was initially converted to undecylenyl bromide. By subjecting undecylenyl bromide to a series of reactions that include azide formation, azide reduction, and reaction with concentrated HCl, we synthesized onium salt with reactive functional group at terminal position was synthesized (refer synthetic scheme in Fig.5). ^1H and ^{13}C NMR and FTIR data support the formation of high purity onium salt [2]. The ^1H NMR spectrum of reactive onium salt (refer to Fig.6) clearly indicates that the vinyl group (peaks at 4.93 δ & 5.78 δ) has been preserved during azide reduction and is available for further reaction with the vinyl ester resin during the formulation of nanocomposites. A description of the synthetic work and product characterization can be found elsewhere [2,3].

A.3 Synthesis of Epoxy Nanocomposite:

The Na clay was ion-exchanged with a mixture of reactive and non-reactive onium salt (25:75 mole% of C-19 amine hydrochloride and C18 amine hydrochloride). We have selected the model resin system DGEBA (provided by Dow Chemical) and

MPDA (meta-phenylene diamine) as the curing agent for the current study. The ion exchanged clay and the epoxy resin were allowed to swell in a reactive diluent, glycidyl methacrylate (GMA). The C19:C18 nanoclay-epoxy nanocomposite was prepared by dispersing C19:C18 ion-exchanged clay in hot DGEBA resin, followed by ultrasonication for about 30 minutes and degassing in vacuum for 2 h. 14.5 phr MPDA was then added to the clay-epoxy mixture. The DGEBA/C19:C18 nanoclay/MPDA mixture was heated for 2 h at 80 °C and post cured for another 2 h at 125 °C. The same curing procedure was used in the formulation of 100% C18 ion-exchanged clay/epoxy nanocomposite.

A.4 Synthesis of Vinyl Ester Nanocomposite:

0.3g of mixed (25% reactive C11 salt : 75% non-reactive C11 salt) clay was soaked in 1.5g of styrene, while 5g of Ashland Apotech Q6055 vinyl ester resin was allowed to swell in 1.0g of styrene. After soaking both organic modified clay and resin in styrene for 3h, both organic modified clay and vinyl ester were combined and sonified on VWR Branson Ultasonifier 250R at 40% duty cycle and at different output controls (from 1 to 10) for 30 minutes. During ultrasonication, the temperature of the mixture was maintained between 30-35°C by placing the reaction vessel in an ice jacket. To the sonified mixture, 0.03 g of N, N dimethyl aniline and 0.06 g of cobalt napthenate (catalyst) were added. The mixture was stirred for 5 minutes after which, 0.12g of methyl ethyl ketone peroxide was added and the mixture was immediately poured into the dog bone mold. The dogbone specimen was precured for 30 minutes at 30°C, post-cured at 100°C for 30 minutes, and cooled gradually in a Lab-Line Instrumentation programmable vacuum oven. The same curing procedure was used towards preparing 100% C11 clay vinyl ester nanocomposite. Additional vinyl ester nanocomposites were also prepared with mixed (75% C18 : 25% C19 salt) clay and pure (100% C18 salt) clay.

B. Formulation of Rubber Filled Nanocomposite

B.1 Synthesis of acrylic rubber dispersion in epoxy resin

The detailed procedure used for the synthesis of acrylic rubber dispersion in epoxy resin can be found elsewhere (4), we briefly outline the steps used in the synthetic scheme. To the preheated epoxy resin (20 g), 0.01 g of ethyl phosphonium acetate and 0.25 g of methacrylic acid was added, and the mixture was additionally heated at 120 °C for 1 h with stirring under nitrogen atmosphere. Then a slurry of 2, 2' azo-bis (2 methyl

propionitrile) (0.2 g) in 2-ethyl hexyl acetate (12.4 g) and glycidyl methacrylate (0.79 g) was gradually added to stirred epoxy resin maintained at 100 °C. The epoxy acrylic mixture was heated for an hour at 120 °C and allowed to attain room temperature. Finally the rubber dispersion in epoxy was placed under vacuum to strip volatile remnants.

B.2 Preparation of cured samples

The detailed procedure for preparation of octadecyl amine hydrochloride functionalized (C18) clay can be found elsewhere [5]. A mixture of C18 clay (0.275 g), epoxy resin (5 g), acrylic rubber dispersant (0.75 g), and tetrahydrofuran (1 g) was sonicated using sonicdismembrator (VWR Branson sonifier 250R) for 30 minutes. Details of the sonication protocol can be found elsewhere [6]. The swelling agent (THF) was stripped from the mixture by placing the sonified mixture in a vacuum oven at 60 °C for 4 h. Then the mixture was allowed to attain room temperature and 5 phr of curative (pyridine) was added and hand mixed. The curative added mixture was poured into dog-bone cavity silicone mold and cured at 120 °C for 16 h using Lab Line Instrumentation programmable oven. The procedure used for the preparation of the cured pristine epoxy, rubber toughened epoxy, and clay filled epoxy nanocomposite samples was similar to that of the rubber dispersed clay filled epoxy nanocomposite.

C Morphological and Mechanical Properties Characterization of Rubber Toughnened Nanocomposite

C.1 XRD and TEM Analysis of Polymer Nanocomposites

XRD analyses were performed using a Scintag Inc. XRG 3000 diffractometer with Cu radiation (40 KV, 35 mA). The scanning speed and the step size were 0.01^0/min and 0.04^0, respectively. The nanocomposite dogbone produced during the molding process has a fairly smooth surface. The dogbone specimens were cut to size and analyzed by XRD.

TEM specimens were cut from dogbone using a ultramicrotome, equipped with a diamond knife. They were collected in a trough filled with water and lifted out of water using 200 mesh copper grids. TEM micrographs were taken with a Philips EM400C at an accelerating voltage of 120 KV.

C.2 Measurement of mechanical properties of cured specimens

The molding process produced dog-bone specimens that are approximately 6 cm (length) by 4 mm (gauge width) by 2 mm (thickness). Tensile experiments were conducted in an Instron tensile tester equipped with 50 kN load cell capability. The experiments were conducted at room temperature using a cross-head speed of 2 mm/min. The stress-strain curves were recorded for 7 specimens of each composition.

RESULTS AND DISCUSSION:

Epoxy Nanocomposite System

Of great interest in this research work is the possibility to control the morphology development of organically modified clay-epoxy nanocomposites by influencing the processing parameters. We examined the role of different mixing techniques such as sonication, diluent-assisted mixing, and the duration of soaking of clay in a diluent on the morphology development of organically modified clay-epoxy nanocomposites. By studying the breadth, position and intensity of the basal reflection of XRD, the relative extent of intercalation/exfoliation of the organoclay-polymer hybrid nanocomposite was determined. Figure 7 is the XRD pattern of nanocomposite for different processing parameters. As can be seen in Figure 7, minimal processing of nanocomposite yields a sharp peak at 2.3^{o} (characteristic of intercalated structure). Soaking clay and polymer in a compatible reactive diluent reduces the intensity of peak, while ultrasonication in combination with soaking further reduces the peak intensity. We noticed that the transparency (a measure of exfoliation) of epoxy nanocomposite with a loading of 3.5 wt% of organically modified clay can be significantly improved upon soaking the resin and clay in 50 phr GMA for 6h and ultrasonication for 30 minutes. Figure 8 is the XRD pattern of nanocomposite as it relates to the amount of diluent. The results indicate that the intensity of the XRD peak corresponding to intercalated clay platelets in the epoxy matrix can be significantly reduced/but not eliminated by adding reactive diluent. In summary, through these results, we demonstrate that a reduction in peak intensity (better dispersion of clay platelets in the polymer matrix) can be achieved when appropriate conditions for processing are considered.

Vinyl Ester Nanocomposite System

The cation exchange capacity (CEC) of Na^+ clay is reported to be 104 mmol/100 g (20). Figure 9 shows the TGA thermograms of Na^+ clay, non-reactive C11 clay, and partially reactive C11 clay. We assign the low percent mass loss at $\approx$ 100 °C to the loss of interparticle water. Thermal decomposition of the ammonium ions in the modified clay is most likely responsible for the drop in weight between $\approx$ 150 °C and 400 °C. Note that this mass loss is absent in the Na clay. As a point of reference, it is worthwhile to mention that pure octadecyl amine hydrochloride has a melting point of 155 °C and thermal decomposition of octadecyl ammonium salt from clay occurs at 210 °C (unpublished data). Recently, Vaia et al., 2001 showed that the onset decomposition temperature for ammonium salt modified organically layered silicate is approximately 155 °C. These observations support our hypothesis that the thermal decomposition of undecyl amine salt should begin at 150 °C. TGA was also performed in air atmosphere to measure the ammonium cation mass fraction in several different samples of treated clay: 87.5 $\pm$ 3.5 mmol/100 g of clay. This value is in general agreement with the reported value.

To confirm the observation that the Na^+ ions have indeed been replaced by undecyl ammonium ions, XRD of the organically modified clay and the Na^+ clay was performed. The d-spacing of the undecyl amine hydrochloride modified clay was found to be 1.40 ± 0.02 nm (for C11 treated non-reactive clay) and 1.39 ± 0.02 nm (for clay treated with a 25:75 mixture of reactive and nonreactive amine, respectively) compared to 1.18 ± 0.02 nm for not-fully-dried Na^+ clay (Figure 10). These values are consistent with complete ion exchange by the organic cation. Specifically, these values indicate that the gallery spacing $t_{gallery}$ after treatment is 0.42 and 0.41 nm, respectively (the thickness of the silicate layer $t_{silicate}$ is 0.98 nm, as determined from fully dried montmorillonite). Assuming complete ion exchange (i.e. f_{cat} = CEC), and no residual water in the gallery, the density of the surfactant-filled gallery, $\rho_{gallery}$, relative to that of the silicate, $\rho_{silicate}$, is:

$$\frac{\rho_{gallery}}{\rho_{silicate}} = f_{cat} M_{amine} \frac{t_{silicate}}{t_{gallery}} \qquad (1)$$

which, in the present case, is 0.43. Here M_{amine} is the molar mass of the ammonium ion. Since the density of the silicate is 2.0 g/cm^3, this corresponds to a reasonable value for the gallery density of 0.86 g/cm^3. Thus, it is likely that complete ion exchange was achieved. Since the uncertainty in $t_{gallery}$ is approximately 5 % (see above), the uncertainty of f_{cat} is likewise. Having achieved essentially complete ion exchange and the resulting increase in d-spacing, further expansion by vinyl ester resin is possible.

After addition and curing of the vinyl ester resin, another peak at $2\theta = 3°$ corresponding to intercalated clay is observed (Figure 11). A small amount of resin lies within the gallery of the treated clay. The position and relative intensity of this peak is sensitive to the conditions used to prepare the composite material. The peak arising from treated clay (at $2\theta = 6.3°$), however, remains prominent and indicates that matrix resin intercalation is not complete.

Although the d-spacing for these two peaks exhibit a ratio of nearly (but not exactly) 2 to 1, we do not interpret the higher order peak as a second order of the first, mainly on account of their relative intensities. If the higher angle peak was a second order, reasonable models for the local electron density predict that the intensity of the second order should be significantly less than the first order. On the contrary, the observed intensity of the higher angle peak is comparable to, and even greater than, that of the low angle peak associated with intercalated clay (giving rise to the peak at $2\theta = 3°$). Therefore, a certain fraction of the clay is intercalated by polymer chain infiltration and certain fraction is nearly as-treated clay, i.e., without polymer chain infiltration (peak at $2\theta = 6.3°$).

Although prior efforts have been made in understanding the kinetic and thermodynamic parameters that control clay platelet separation, many issues associated with the processing conditions as it relates to control of morphology remain unresolved. In this study, we consider some (thermodynamic) parameters (ultrasonication and the use of a swelling agent) that may promote diffusion of vinyl ester resin into the clay interlayer. To assess the role of the terminal functional group in promoting intercalated/exfoliated structure, the XRD patterns of partially reactive and non-reactive C11 clay nanocomposite were also compared.

The relative amounts of exfoliated, intercalated, and as-treated clay and the size of clay particle aggregates depend significantly on composition and processing, according to XRD and TEM analysis. It appears also that the presence or absence of reactive amines influences the morphology. Weak, hand mixing produces a poor dispersion, and the composite material is turbid. TEM micrographs reveal large, 1to10 μm aggregates (see Figure 12a), the evidence for poor dispersion. A very small fraction of isolated, exfoliated silicate sheets are also observed. The great majority of silicate layers lie within the aggregates, and XRD reflections arising from intercalated and as-treated clay are observed (Figure 11). Low-power sonication and heating before polymerization does little to change the morphology; both XRD peaks remain essentially unchanged, with only slight sample-to-sample variations in the peak positions (± 0.2°) and relative intensity.

Addition of a co-monomer styrene and high intensity ultrasonic mixing favor intercalation and exfoliation. Since mass transport of highly viscous resin into clay galleries is widely considered one of the limiting steps to exfoliation, the use of low viscosity diluent and ultrasonication may indeed facilitate resin transport. Styrene was chosen as the swelling agent and reactive diluent because it is widely used in vinyl ester preparation. The clay and vinyl ester were premixed with styrene to obtain a low-viscosity suspension in which efficient mixing of the various components can be achieved. While styrene alone does not significantly change the d-spacing of the intercalated structure, the intensity of the intercalated clay peaks is reduced (Figure 11). Some reduction is expected simply on account of the lower concentration of silicate in the sample[2] an increased fraction of exfoliation causes further reduction in diffraction intensity at 3 and 6.3°. TEM micrographs of the composite show many more small particles (aggregates) and some individual plates. Large aggregates persist, and the composite remains turbid.

Much-higher-power sonication breaks these large aggregates and produces a more uniform dispersion of small aggregates (typically several layers in thickness) and exfoliated particles (Figure 12b), and the composite is comparatively more transparent. It

[2] The mass fraction of treated clay in nanocomposite without styrene is approximately 5 % and nanocomposite with styrene is approximately 4 %.

is also reported that in polystyrene nanocomposite, sonication improves dispersion of clay platelets. The high-power ultrasonifier generates ultrasonic waves of high amplitude that induce cavitation bubbles as small as 0.01 μm. It is conceivable that these highly energetic bubbles when they form in the gallery spaces can induce deagglomeration of clay platelets. It is commonly reported in the literature that when the clay platelets are sufficiently separated and mixed with resin, often the viscosity of the system increases at low shear rates. In our study, we noticed an increase in the viscosity during and at the end of ultrasonication. This increase in viscosity arises because as the dispersion improves, the effective volume of clay platelets dramatically increases (consistent with TEM images, Figure 12).

Finally, treatment of the clay with the reactive amine produces the highest degree of exfoliation. When the high-power sonication was not used, and/or in the absence of styrene co-monomer, both as-treated and intercalated XRD peaks were observed (Figure 11), as before. These results are consistent with TEM images. Figure 13 showing the TEM micrographs of polymer nanocomposites containing a) RC11, no styrene with low-power sonication and b) RC11, styrene with low-power sonication is provided. However, when high-power sonication was used to mix samples with styrene co-monomer (Figure 12b and 12c), the intercalated fraction decreased, and the composite is more transparent. Nevertheless, a fraction of as-treated clay remains in these composites; aggregates are small (several silicate layers) and dispersed uniformly (Figure 12c). Most exfoliated silicate particles are not observed edge on, so they appear as ribbons in these thin sections. Reaction of as-treated clay is not likely because of steric constraints, and the as-treated clay remains aggregated. Within the slightly expanded gallery of the intercalated clay, copolymerization of either vinyl ester or styrene with vinyl amine surfactant is possible, and the reaction could further promote exfoliation of these silicate layers.

To establish that the fraction of clay aggregates remaining in the nanocomposites depends on the chain length and functional group of the reactive onium salt used in functionalizing clay, we compared the TEM micrographs of partially reactive long chain and medium chain organoclay nanocomposites. It should be mentioned that the C19 onium ion has olefinic functionality at the mid point of the alkyl chain while the C11

onium ion has olefinic functionality at the terminal end of the alkyl chain and the C19 salt has hydroxyl group along the backbone chain while C11 onium ion lacks hydroxyl group. It should also be noted that the vinyl ester has hydroxyl functional groups along the backbone of the oligomeric chain and consequently the hydroxyl groups present in the reactive salt of long chain functionalized clay may enhance the miscibility of the matrix resin when C18 / C19 clay used, by promoting the diffusion of resin in the clay gallery. We observe considerable differences in the images 14 (b) and 14(d). In Figure 14d there are ribbons of clay aggregates while in Figure 14b there are far fewer ribbon aggregates. Furthermore, the average aggregate size (stacked clay platelets) is much smaller in C18 / C19 clay nanocomposite compared to that of its medium chain counterpart. This further supports our observation that the degree of exfoliation is greatly dependent on the length of alkyl onium salt used in functionalizing clay. TEM micrographs suggest that apart from location of the olefinic group or availability of hydroxyl group on the surfactant, the chain length of the surfactant is a major factor in formulating highly dispersed clay nanocomposite. Similar trends in clay platelet separation were noticed for nonreactive long chain and nonreactive medium chain surfactants based nanocomposites. By comparing, medium and, long chain length partially reactive and, nonreactive onium salts functionalized clay nanocomposites, this study has established that the clay platelet exfoliation is indeed dependent on the chain length and chemistry of onium salt used for functionalizing the clay.

An Explanation to Formation of Exfoliated Nanocomposite:

In clay filled resin, the layer separation and polymer network formation steps control the final morphology of nanocomposite. For formulating exfoliated nanocomposite, either the network structure of resin has to occur concurrently as the clay layer separates or layer separation should precede the network structure formation. For layer separation to occur while the network structure is being formed, the rate of layer separation must be considerably faster than the kinetics of the bulk network structure formation. To enhance the rate of gallery separation, generally the chemistry of organic modifiers on the exchanged clay surface is made compatible to the resin being investigated. The fundamental assumption is that organic modifiers can participate in the reaction(s) with resin components and improve the miscibility of the clay with resin.

Specific associations between the functionalized clay and epoxy resin have been proposed in the formulation of epoxy nanocomposite. For example, it is assumed that the olefinic group in the undecenyl amine functionalized clay can react with styrene and/or vinyl ester resin, and/or combination thereof. The intragallery reaction rate and the structural composition of network resin between the layer may well depend on the reactivity of the local components in clay layer spacing. One can envision the formation of copolymer structures, homopolymers, and hybrid (clay/polymer interface) structure within the gallery. The characterization of vinyl ester nanocomposite to establish the coupling of surfactant-treated clay, comonomer, and/or matrix resin is a difficult and complex issue. In an attempt to address the chemical bonding aspect of chemically functionalized clay/vinyl ester nanocomposite, we performed a model experiment to study the reactivity of reactive salt with styrene. Preliminary NMR data indicate (by loss of alkenyl-proton signal) that the reactive salt copolymerizes with styrene monomer or homopolymerizes itself (work in progress). Indirect evidence for the bonding between reactive clay and resin can also be obtained by observing an increase in viscosity of the clay/resin mixture and improvement in the stiffness and strength of nanocomposite. In our forthcoming article, we describe the mechanical property enhancement of reactive clay (hydroxyl and olefinic functional C19 amine hydrochloride surfactant-treated montmorillonite clay) vinyl ester nanocomposite over nonreactive C18 clay vinyl ester nanocomposite and pristine resin (7).

In addition to the role of the partially reactive clay towards resin, there are kinetic and thermodynamic parameters that have to be considered in promoting exfoliation of clay platelets in vinyl ester resin. The addition of low viscosity reactive monomer (styrene) generally facilitates the transport of higher viscosity resin in the gallery spacing, and also improves the swelling the clay platelets because of nonpolar-nonpolar interactions (between the olefinic group in undecenyl amine functionalized clay and olefinic group in styrene). The transport of resin and comonomer in the gallery spacing of clay can be further facilitated by the use of an effective mixing technique. High-power sonication can effectively induce deagglomeration of clay platelets in the presence of low viscosity reactive diluent.

Mechanical Properties of Nanocomposites

Table 1 summarizes the mechanical properties of vinyl ester nanocomposite. The modulus, strength, and elongation at break values for vinyl ester filled with C18 clay and C18 / C19 clay were compared with that of unfilled cured vinyl ester resin. For the individual sample type, the standard deviation is mentioned within the paranthesis. A minimum of seven samples was tested for individual compositions. To determine whether there were statistically significant differences in the average strength, modulus and elongation at break due to the addition of functionalized clay to vinyl ester resin, pooled standard deviation was used. Table 2 summarizes the difference in modulus, strength, and elongation at break due to the addition of nonreactive and partially reactive clay to vinyl ester resin. Any confidence level lower than 95 % was equivalent to no statistically significant difference. For example, Table 2 shows that there is 17 % improvement in the modulus value for C18 / C19 clay filled nanocomposite when compared to that of unfilled resin. Based on pooled standard deviation calculation, the improvement is statistically significant at a confidence level of 95%. Similar analysis was extended to compare the modulus of other nanocomposite system. It was found that the modulus of C18 / C19 clay filled vinyl ester nanocomposite is greater than that of C18 clay filled vinyl ester nanocomposite which in turn is greater than unfilled resin. At an organoclay loading of 3.5 wt % (montmorillonite content of about 2.5%), the modulus improved by ~20 % for C18 / C19 clay dispersed nanocomposite, while the modulus improved by ~10 % for C18 clay dispersed nanocomposite compared to that of unfilled cured resin. Our method of functionalizing clay with long chain partially reactive onium salt has yielded improvement in modulus of nanocomposite at a montmorillonite content of only 2.5 wt % which is similar to the literature reporting of improvement in modulus of chemically functionalized unsaturated polyester nanocomposite.

Table 1 also compares the tensile strength of nanocomposites formulated with C18 clay and C18 / C19 clay to that of unfilled cured resin. Our mean data may indicate that the C18 / C19 clay in vinyl ester resin may have higher strength value than the respective counterpart. However, there is considerable % of uncertainty in the data, making the reported differences in the mean strength values statistically insignificant (refer Table 2). We believe that the uncertainty associated with strength data is because

of the anisotropy of the nanocomposite material. The anisotropic nature of the material could be a result of the orientation of clay platelets, chemo-rheological difference at nanoscale domain level, variation in the network structure of resin within the clay gallery to that of the bulk resin, and the extent of clay polymer bonding at the interface. Similar explanation has been proposed to describe the findings in coupling agent modified montmorillonite reinforced unsaturated polyester resin nanocomposite.

The elongation at break of vinyl ester resin reinforced with C18 clay and C18 / C19 clay was found to be considerably better than that for unfilled resin. The results in Table 2 demonstrate that small improvements in elongation at break of vinyl ester resin can be obtained with the addition of C18 clay and C18 / C19 clay filler. In summary, the tensile test results indicate that the strength and modulus improvement of vinyl ester nanocomposites can be achieved when montmorillonite clay is modified with long chain partially reactive (C18 / C19) onium salts. Similar trend in the results were observed for partially reactive organoclay filled epoxy resin nanocomposites (data not published).

Rubber Filled Nanocomposite System

As mentioned earlier for vinyl ester nanocomposites and epoxy nanocomposites, the strength and modulus of nanocomposite is higher than that of resin system with diluent. However, the failure strain of the nanocomposites are reduced to some extent. The observations suggest that strategies to improve the failure strain of nanocomposites may include addressing the fracture toughness / failure strain of the resin. In this study, we use rubber dispersion technology to improve the failure strain of clay filled epoxy resin.

Typical examples of the stress-strain plots of the epoxy, rubber modified epoxy, rubber dispersed clay filled epoxy, and clay filled epoxy for systems containing 15 phr rubber concentration and organoclay amount of 5.5 phr, are shown in Figure 15. The pristine epoxy shows a failure behavior characteristic of brittle material. The load increases linearly with displacement to a maximum value, at which point there is evidently catastrophic failure of the specimen. In clay filled epoxy specimen, the load carrying capability of the nanocomposite is far higher than the epoxy resin studied. After yielding, we observe distinguishable drop in load that is accompanied by minor load

stabilization feature followed by failure of specimen; which was not observed in the epoxy specimen. This may be a result of the stress transferring ability of fairly percolated clay platelets arrangement in the epoxy matrix. In rubber dispersed epoxy, the failure behavior has a smooth transition from a region where the load increases linearly with displacement to a maximum value and yielding which is followed by failure of specimen. In our previous study, we showed that at 15 phr rubber dispersed in epoxy, the crack growth is very stable before and after the maximum load. Associated with this type of stress-strain behavior, there was a distinct region of stress whitened region over a fraction of the gauge length of the test specimen. The stress-strain plot for rubber dispersed clay filled epoxy specimen also exhibits a smooth transition in the plot before and after the load reaches the maximum value. The plot has features that resemble that of rubber modified epoxy, despite the addition of clay platelets to resin system. Furthermore, the sample showed considerable amount of stress-whitened region an indication of crazing mechanism under stressed condition.

Table 3 summarizes the mechanical properties of cured epoxy system. For the individual composition type, the standard deviation is mentioned within the paranthesis. When clay particles were added to epoxy, an improvement in modulus was noticed which is consistent with previously reported observations of nanocomposites, while when rubber dispersants were added to epoxy, a reduction of modulus and strength and an improvement in the failure strain was noticed over the pristine epoxy. As mentioned previously, the addition of rubber dispersants and nanoclay filler to pristine epoxy provides the most striking data. The results clearly show that the loss in modulus and strength resulting from the addition of rubber dispersants to epoxy is offset by the addition of clay while the marginal loss of failure strain resulting from the addition of clay to epoxy is offset by the addition of rubber dispersants to the nanocomposite. At 15 phr concentration of rubber dispersant, the failure strain was found to be consistently higher than that of rubber dispersed epoxy. The most commonly accepted explanation for improvement in failure strain of rubber toughened epoxy is that the rubber particles act to initiate and assist yielding and plastic flow in the epoxy material. However, the failure strain data suggest that in addition to the widely accepted explanation there may

be other mechanisms (e.g. stress transfer) prevailing in clay filled rubber dispersed epoxy nanocomposite.

To examine the failure mechanism, the fracture surfaces for the three different samples were examined by SEM. Figure 16 shows the typical results of SEM images of the fracture surfaces of the epoxy system. The fracture surface of the clay filled epoxy (Figure 16a) showed considerable roughness in certain regions of the sample, similar to that observed for unsaturated polyester clay nanocomposites. It is commonly reported that the additional surface area (as noticed by rougher region) is created by the presence of clay platelets in the nanocomposite sample. To study the distribution of clay platelets in the epoxy matrix, TEM examination was performed on the ultramicrotomed specimen. Figure 17 shows TEM micrograph of clay filled epoxy nanocomposites with and without rubber dispersant. We notice that in the sectioned samples of C18 clay epoxy nanocomposite, the clay aggregates are fewer and are well dispersed in the epoxy matrix than the pristine clay dispersed epoxy nanocomposite (data not shown). The degree of dispersion of the clay platelets in matrix was found to be sensitive to the chemistry associated with clay platelet modification and processing conditions (8). A word of caution, we do notice some regions in the sectioned sample where the clay platelets retain their face to face orientation and their original alignment. For this reason, we interpret the micrograph as a section of a partially delaminated nanocomposite. The improved dispersion of clay platelets in resin matrix manifests itself in the crack diversion and alteration of crack pathway. The formation of rougher area correlates with improvement in mechanical properties of nanocomposites.

Microscopic examination of fractured rubber modified epoxy sample (Figure 16b) shows considerable yielding and plastic deformation and a large number of holes where the rubber particles have cavitated. In some of the holes, the rubber particles can be seen suggesting failure at the epoxy matrix-rubber particle interface. Like the rubber dispersed epoxy, the fractured surface of rubber dispersed epoxy nanocomposite (Figure 16c) shows considerable yielding and plastic deformation. Furthermore, it should be mentioned that the roughness of the sample is higher in rubber dispersed nanocomposite compared to rubber toughened epoxy. We notice holes in the fractured specimen that are a result of cavitation of rubber particles. We infer that a number of mechanisms i.e.

stress transferring capability of individual clay platelet, rubber particle cavitation, plastic flow and yielding of the matrix initiated by the rubber particle, contributed in improving the failure strain of rubber dispersed clay nanocomposite (9).

Through TEM observation, the distribution of clay platelets and rubber particles in the nanocomposite (Figure 17b) was examined. The micrograph shows dispersion of clay platelets and rubber particles (average size 200 nm) in the epoxy matrix. At 15 phr rubber concentration, there is no evidence of phase inversion of rubber particles (retention of particulate morphology) in the epoxy matrix. As mentioned previously, the morphology of clay platelets in nanocomposite can be best described as partially delaminated. We notice that the clay sheets tend to align around the walls of rubber particle, this may assist the particles to withstand additional stretching forces before failure occurs at the epoxy matrix-rubber particle interface. It may be that the aligned clay particles are acting as additional reinforcement to protect the interface from external stretching force. A similar explanation has been proposed to describe improvement in properties of polypropylene-clay nanocomposite foams prepared using supercritical CO_2 as foaming agent.

Summary

We have shown that the choice of the organic treatment and proper mixing techniques can significantly influence the clay platelet separation and the dispersion of clay platelets in the vinyl ester resin matrix.

1. Vernonia oil based long chain onium surfactant was effectively used to modify montmorillonite clay for nanocomposites applications.

2. The relative amounts of exfoliated, intercalated, and as-treated clay and also the size of clay aggregates depend on the chemistry and chain length of the onium salt used in functionalizing clay and processing conditions. Addition of a co-monomer styrene and high intensity ultrasonic mixing favor intercalated and exfoliated clay platelet morphology.

3. TEM micrographs show uniform dispersion of clay platelets in the vinyl ester matrix for long chain partially reactive functionalized organoclay filled vinyl ester nanocomposite.

We have noticed that the strength and modulus of long chain partially reactive functionalized organoclay filled vinyl ester nanocomposite is higher compared to the long chain nonreactive functionalized organoclay filled vinyl ester nanocomposite and unfilled cured vinyl ester resin.

We have demonstrated the symbiotic relationship between clay platelets and rubber dispersants in improving the strength, modulus, and failure strain of rubber dispersed epoxy nanocomposite. Plausible mechanism for improved failure strain of rubber dispersed clay filled nanocomposite may include stress transfer capability of clay platelets, rubber particle cavitation and plastic flow and yielding of matrix initiated by the rubber particles.

REFERENCES:

1. S. Balakrishnan and D. Raghavan, Synthesis of 13(14) Hydroxy-cis-10-Nonadecenyl amine hydrochloride, *Journal of the American Oil Chemists Society*, 80(5), 503(2003).

2. D. Yebassa, S. Balakrishnan, E. Feresenbet, D. Raghavan, P. R. Start, and S. D. Hudson, Chemically Functionalized Clay Vinyl Ester Nanocomposites : Effect of Processing Conditions, *J. Polym. Sci. Polym. Chem. Edn.*, 42, in print (2004).

3. D. Yebassa, S. Balakrishnan and D. Raghavan, Next Generation Nanocomposites Through Nanotechnology, NANOTECH 2003, 260-263 San Francisco, CA.

4. J. He, D. Raghavan, D. Hoffman and D. Hunston, The Influence of Elastomer Concentration on Toughness in Dispersions Containing Preformed Acrylic Elastomeric Particles in an Epoxy Matrix, Polymer, 40, 1923(1999).

5. S. Balakrishnan and D. Raghavan, Chemically Functionalized Clay Epoxy Nanocomposites for Aerospace Applications, NANOTECH 2003, 263-266, San Francisco, CA..

6. D. Raghavan, S. Balakrishnan and Y. Gebrekristios, Optimizing Processing Conditions to Influence the Morphology of Nanocomposites, NANOTECH 2003, 3, 243(2003).

7. S. Balakrishnan and D. Raghavan, Chemically Functionalized Clay Vinyl Ester Nanocomposite II. Vernonia Oil Based Surfactant, *Journal of Reinforced Plastics and Composites*, in print(2004).

8. S. Balakrishnan and D. Raghavan, Mechanical Properties of Chemically Functionalized Clay Vinyl Ester Nanocomposites, MRS Proceedings on *Mechanical Properties of Nanostructure Materials and Nanocomposites*, Boston, MA, in print 2004.

9. S. Balakrishnan and D. Raghavan, Acrylic Elastomeric Particle Dispersed Epoxy-Clay Hybrid Nanocomposite : Mechanical Properties, Macromolecular Rapid Communication, *Macromolecular Rapid Communication*, 25, 481(2004).

Table 1: Summary of Tensile Test Result for Cured Vinyl Ester Samples

Type of Material	Tensile strength (MPa)	Tensile modulus (MPa)	Tensile strain (%)
Unfilled cured vinyl ester	93.22 (8.9)	2251 (74.3)	5.02 (0.52)
Vinyl ester with 100 % long chain non-reactive C18 clay nanocomposites	99.0 (7.8)	2465.6 (160.2)	5.75 (0.48)
Vinyl ester with long chain partially reactive C18 / C19 clay nanocomposites	104.3 (8.2)	2710 (100.03)	6.1 (0.32)

Table 2: Difference in mean tensile property values for cured vinyl ester resin and nanocomposite samples.

Material type and nano filler level	Difference in property values (%)	Confidence level (%) ***
Tensile modulus		
75:25 – N	17**	95
100 – N	9	95
75:25 - 100	9	95
Tensile strength		
75:25 – N	10.7	*
100 – N	6	*
75:25 - 100	5.1	*
Tensile strain		
75:25 – N	17.7	95
100 – N	12.7	95
75:25 - 100	5.7	*

100 – Vinyl ester nanocomposites made with 100 % C18 clay
75:25 - Vinyl ester nanocomposites made with 75:25 C18 / C19 clay
N – Unfilled cured vinyl ester sample
* Not statistically different (confidence level <90%)
** 75:25 – N = the difference in the mean tensile modulus value divided by 75:25 sample tensile modulus and the resultant value multiplied by 100
*** Confidence level at which the two means are different

Table 1: Summary of tensile test result for cured epoxy samples

Type of Material	Tensile strength (MPa)	Tensile modulus (MPa)	Tensile break strain (%)
Epoxy resin	160.5 (3.1)	2256.5 (90.1)	8.3 (0.7)
[a]Clay nanocomposite	177.5 (4.8)	2775.9 (60.1)	8.2 (0.43)
[b]Rubber dispersed epoxy	143.3 (1.32)	1976.2 (106.9)	9.98 (1.0)
[a,b]Rubber dispersed clay nanocomposite	161.1 (4.8)	2352.8 (85.1)	11.5 (0.6)

a – 5.5 phr C18 clay

b –15 phr acrylic rubber dispersant

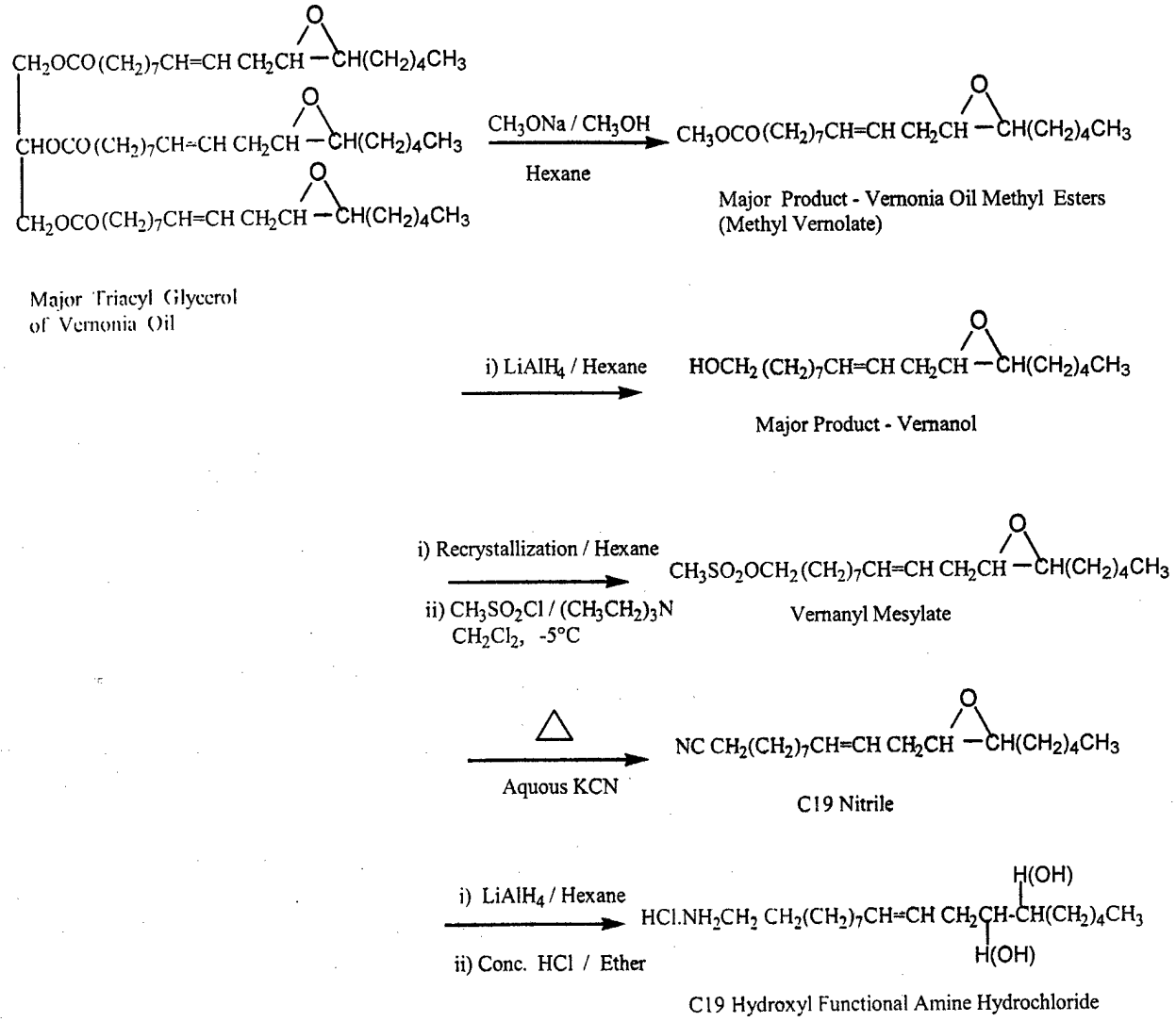

Figure 1 : Reaction scheme for the formation of C19 Hydroxyl Functional Amine Hydrochloride

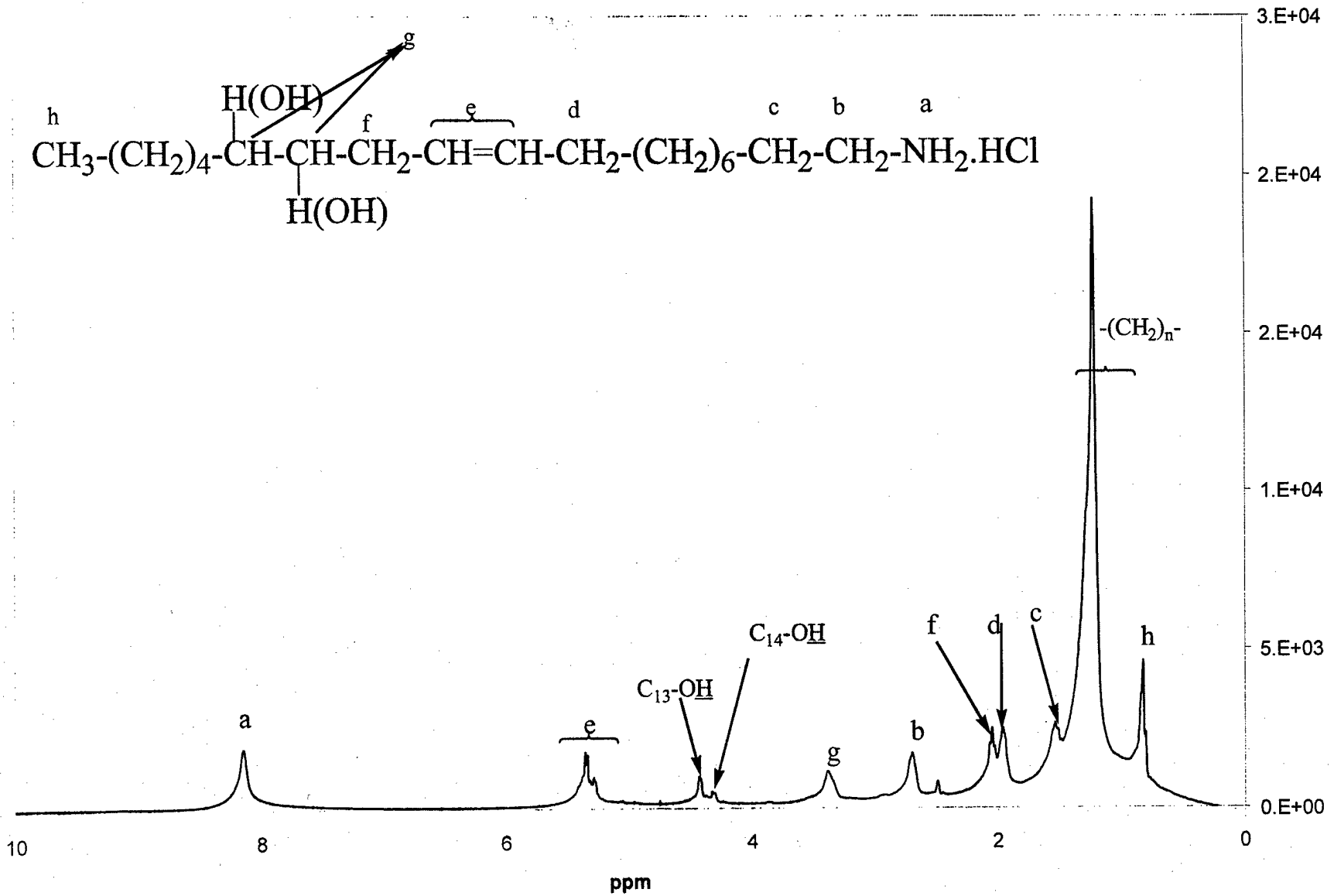

Figure 2 : Proton NMR of C19 Hydroxyl Functional Amine Hydrochloride

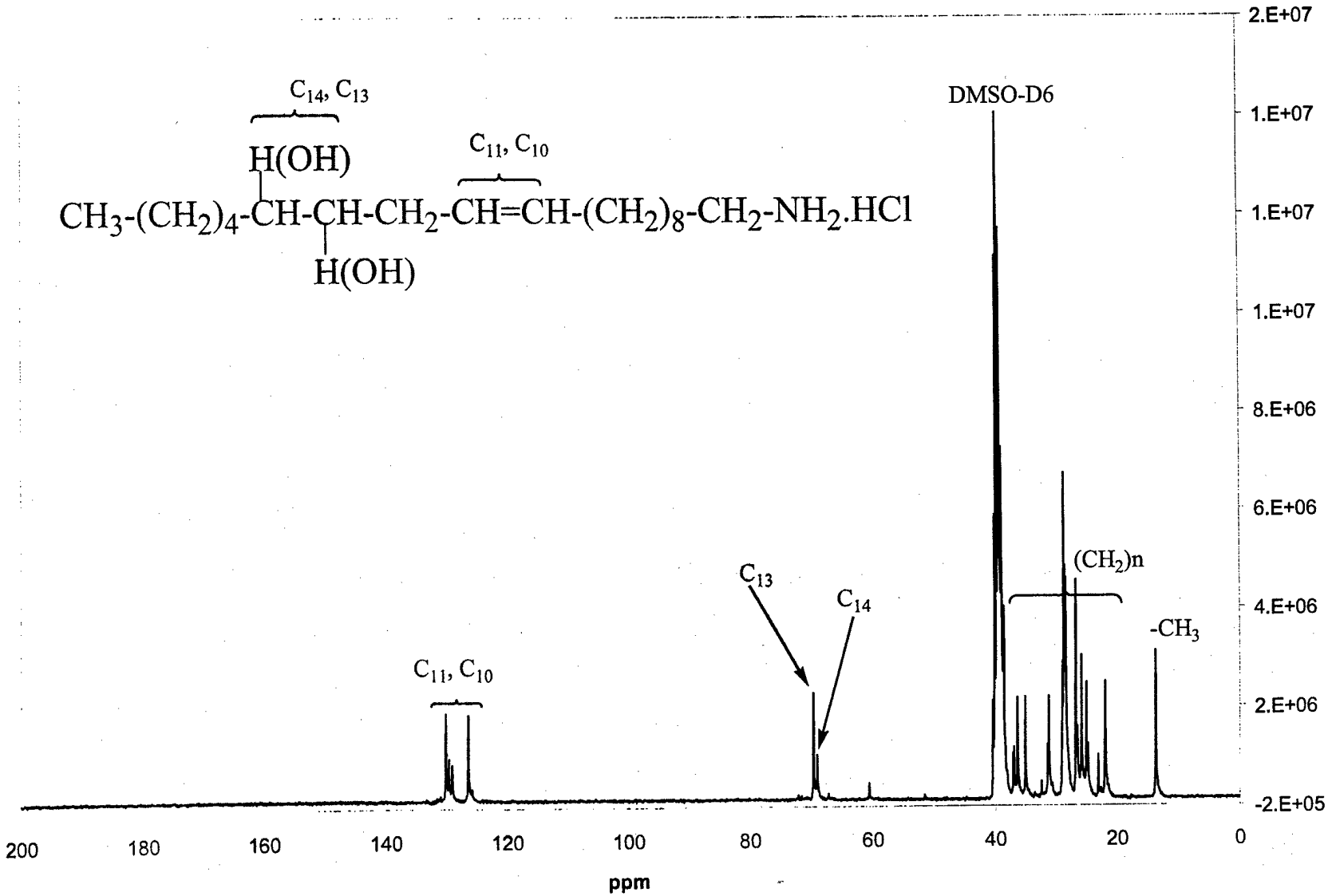

Figure 3 : Carbon (13) NMR of C19 Hydroxyl Functional Amine Hydrochloride

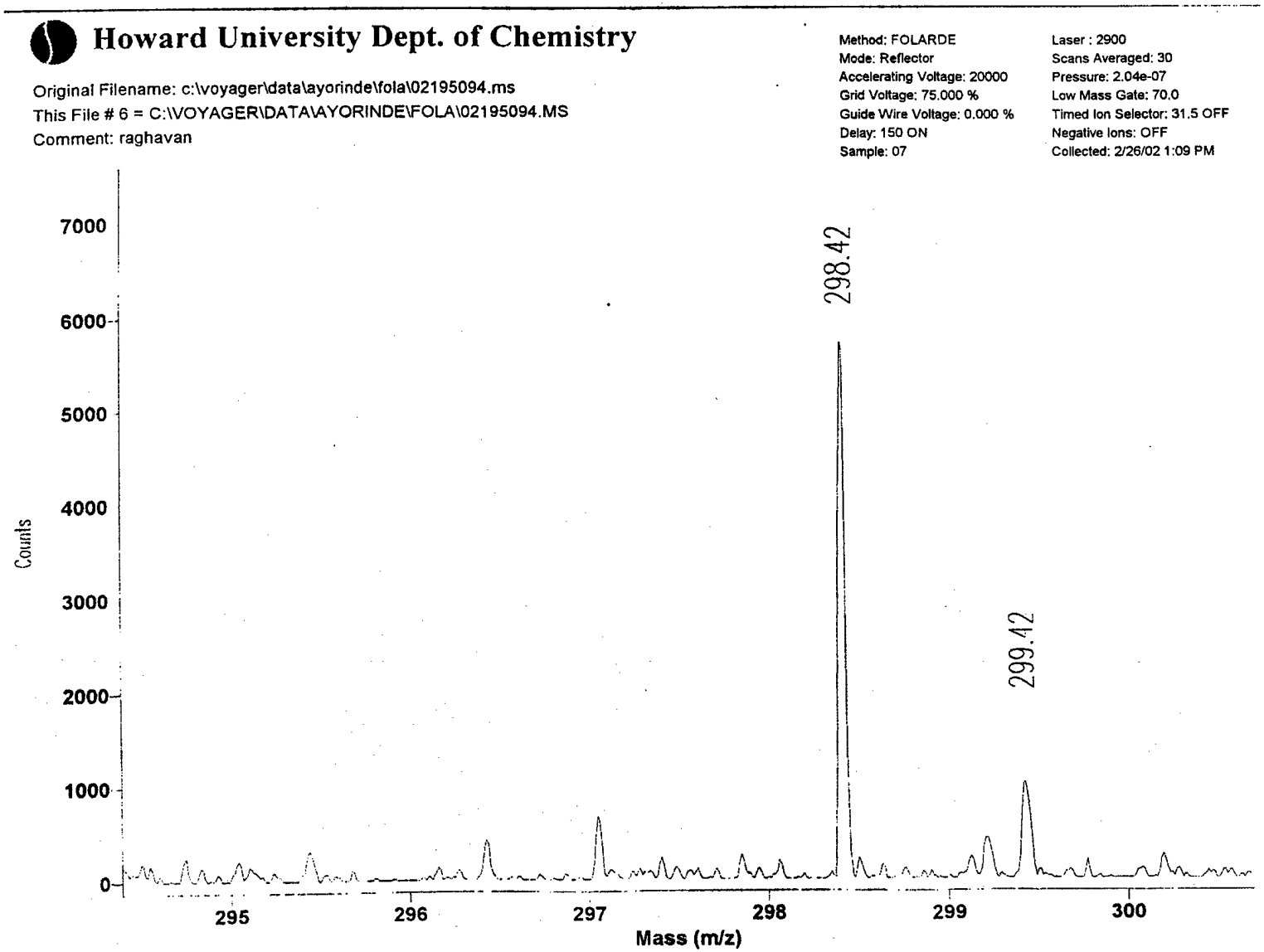

Figure 4 : MALDT Spectrum of C19 Hydroxyl Functional Amine Hydrochloride

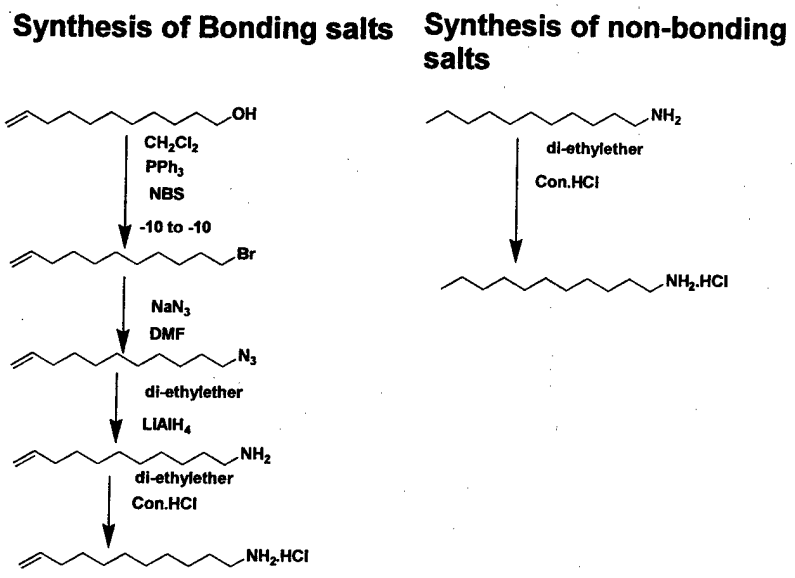

Figure 5. Reaction scheme for synthesizing undecenyl amine hydrochloride and undecyl amine hydrochloride.

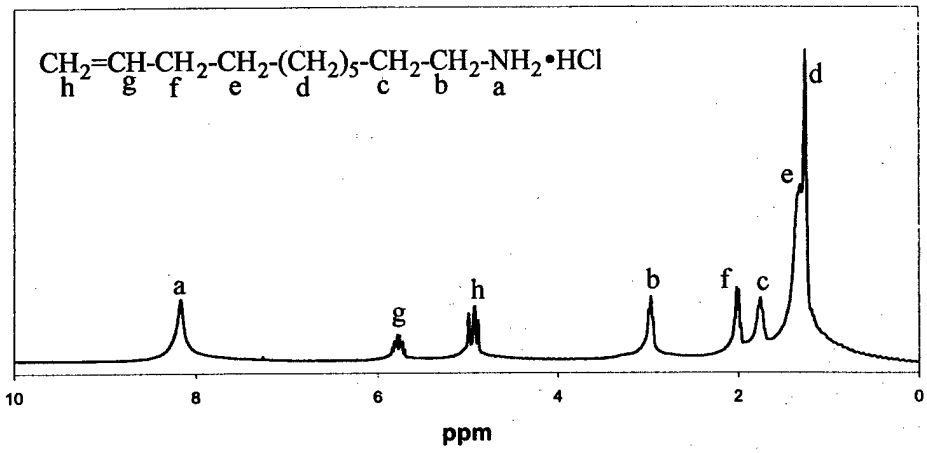

Figure 6. ^{1}H NMR spectrum of undecylenyl amine hydrochloride.

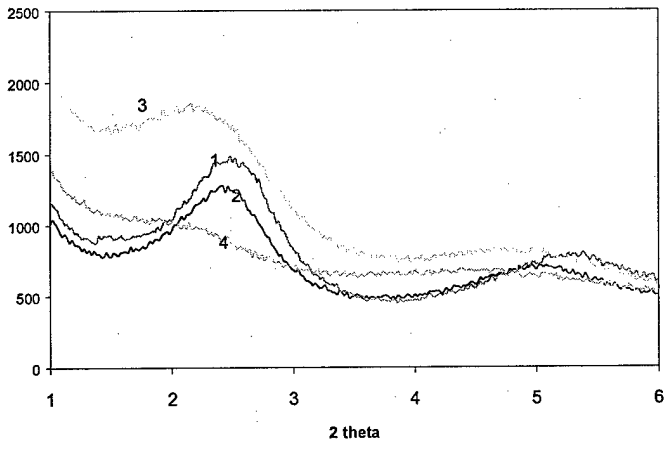

Figure 7 Figure 1: XRD pattern of nanocomposite for different processing parameters; 1. No sonication and no soaking, 2. Three hour soaking, 3. Sonication, 4. Three hour soaking and sonication, 5. Six hour soaking and sonication

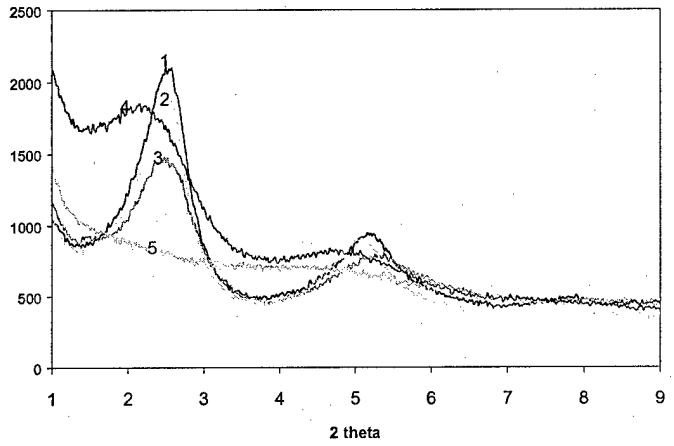

Figure 8: XRD pattern of nanocomposite at different reactive diluent concentrations; 1. Zero phr GMA, 2. 30 phr GMA, 3. 50 phr GMA and 4. 60 phr GMA.

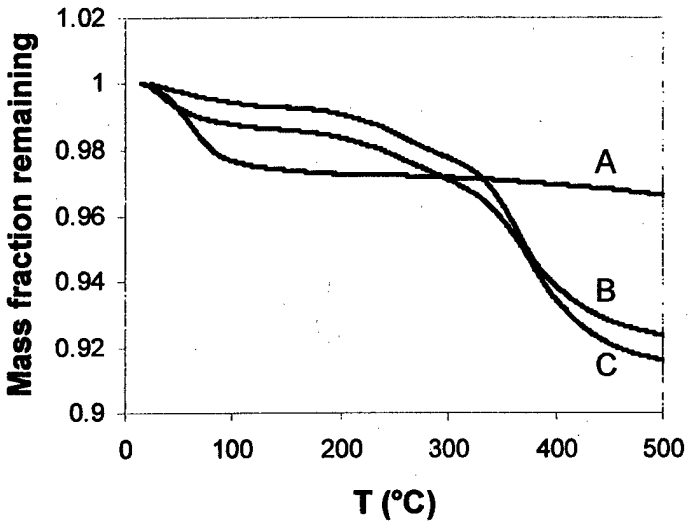

Figure 9. TGA analysis of a) Na^+ clay, b) nonreactive C11 clay, NC11, and (c) reactive C11 clay, RC11.

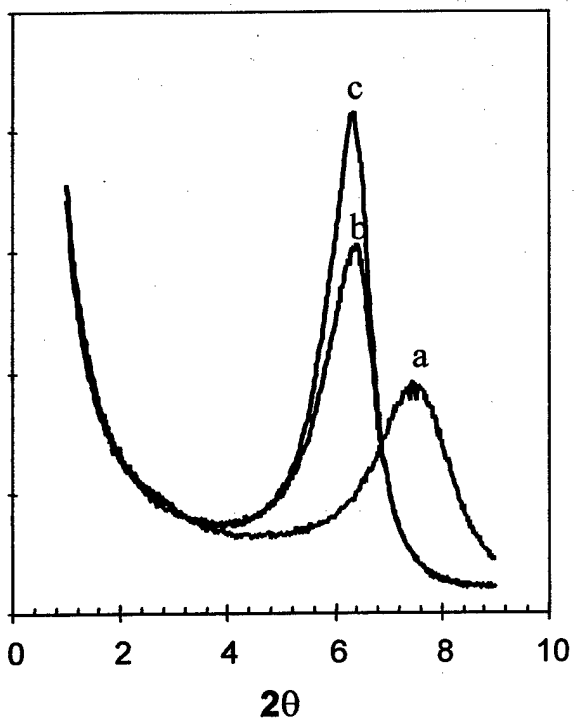

Figure 10. XRD of a) Na^+ clay, b) NC11 clay, and c) RC11 clay.

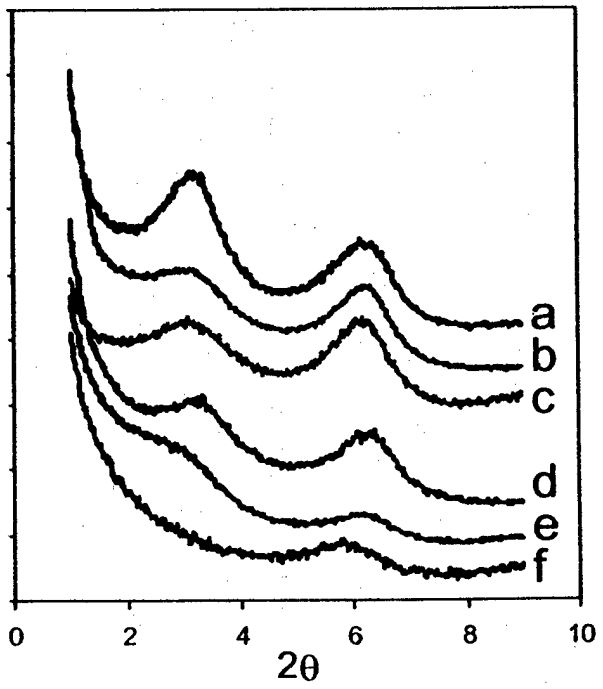

Figure 11. XRD of polymer clay composites. The peak at approximately 6.3° is associated with as-treated clay (see Figure 6), and the peak at approximately 3° is associated with clay that is intercalated with resin. a) NC11, no styrene, low power. b) NC11, no styrene, high power. c) NC11, styrene, high power; the peaks are less intense. d) RC11, no styrene, low power. e) RC11, styrene, low power; less intense diffraction. f) RC11, styrene, high power; peak associated with intercalated structure is absent.

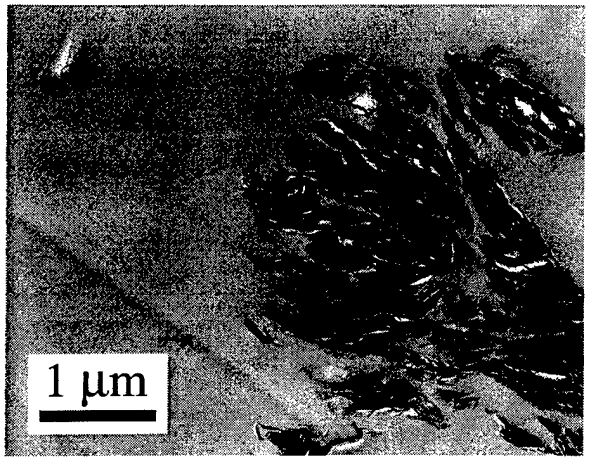

(a)

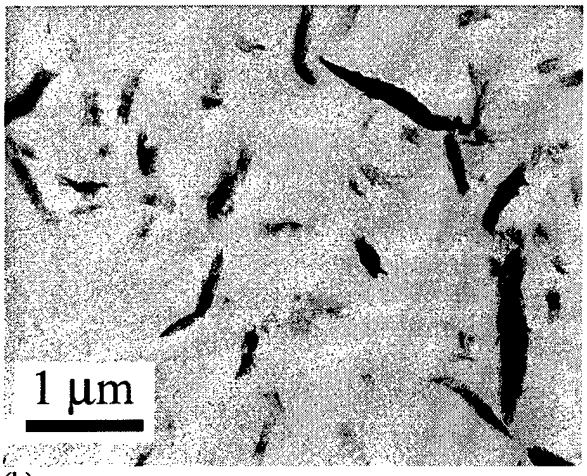

(b)

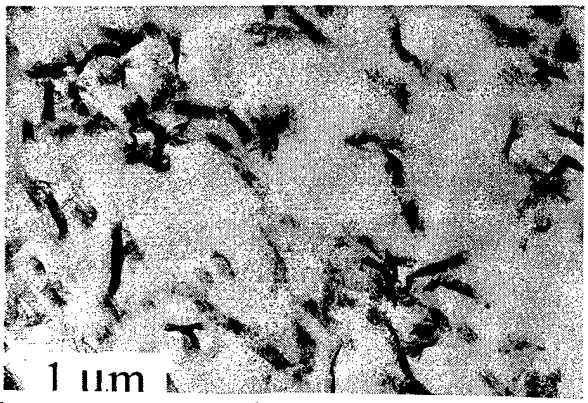

Figure 12. TEM micrographs of composite morphology. a) NC11 no styrene, low power; large aggregates are scattered throughout the sample, and only a few individual (exfoliated) silicate plates are observed; compare Figure 11a b) NC11, styrene, high power; small aggregates are well dispersed, and the exfoliated fraction is higher; compare Figure 11c c) RC11, styrene, high power; compare Figure 11f. Images (b) and (c) are similar, because aggregates of intercalated and as-treated clay are similar. The average aggregate size is slightly smaller in (c), and the degree of exfoliation is greater. Most exfoliated silicate particles are not observed edge on, so they appear as ribbons in these thin sections.

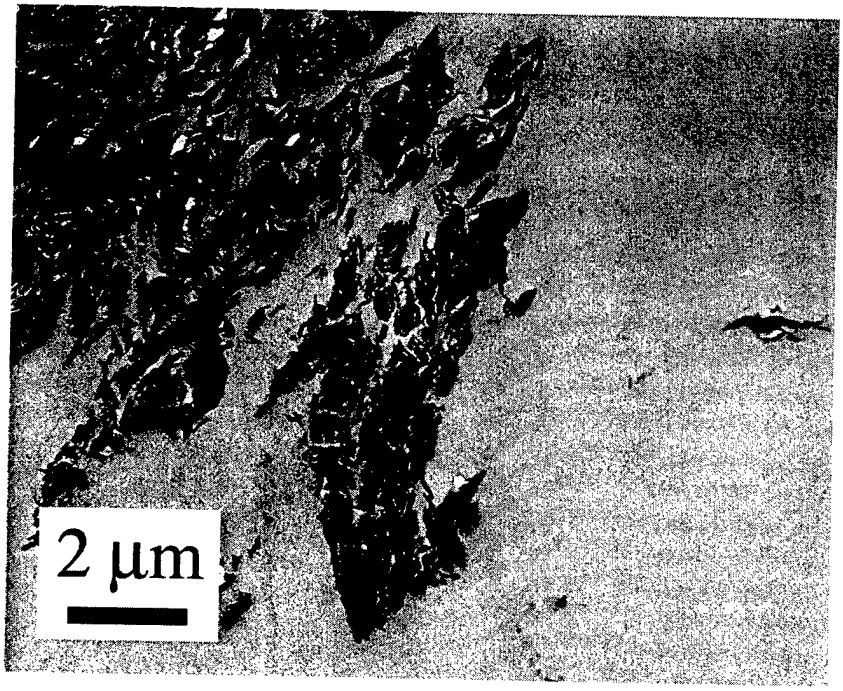

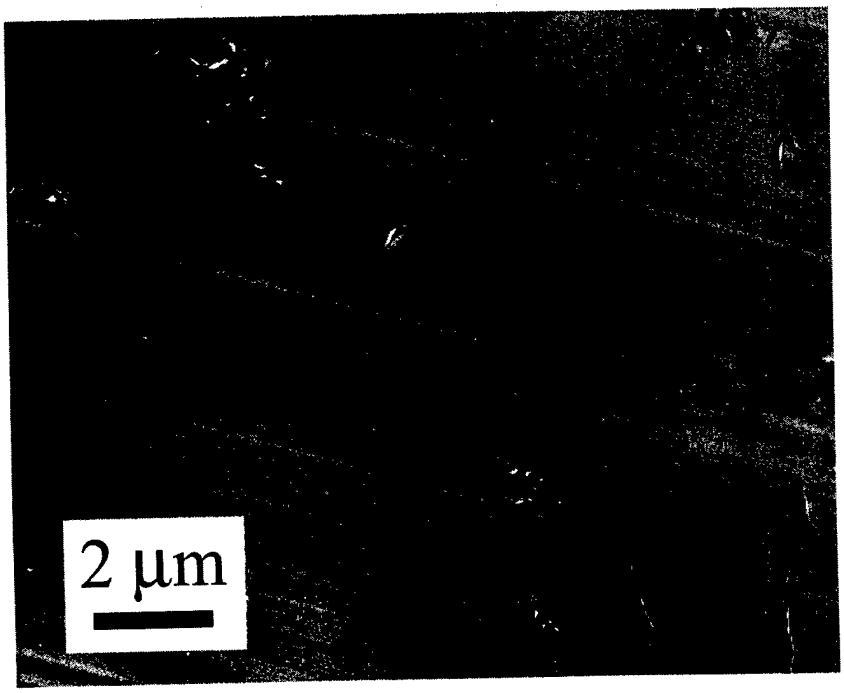

Figure 13 TEM micrographs of composite morphology a) RC11, no styrene, low power (cf. Figure 11d) and b) RC11, styrene, low power (cf. Figure 11e).

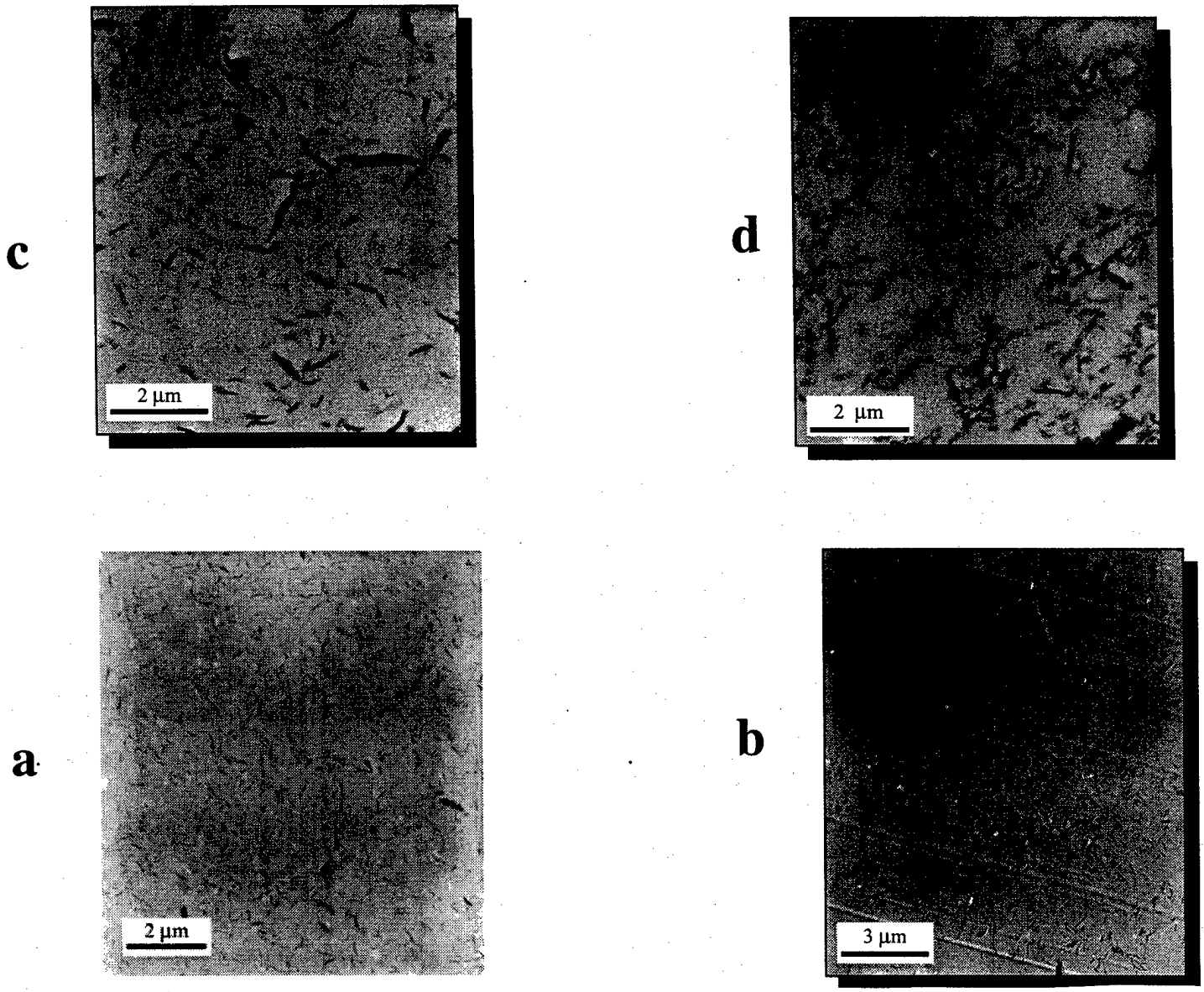

Figure 14 TEM micrographs of vinyl ester nanocomposite morphology. Nanocomposite was formulated using (a) long chain nonreactive C18 clay, (b) long chain partially reactive C18 / C19 clay, (c) medium chain nonreactive C11 clay and (d) medium chain partially reactive C11 clay.

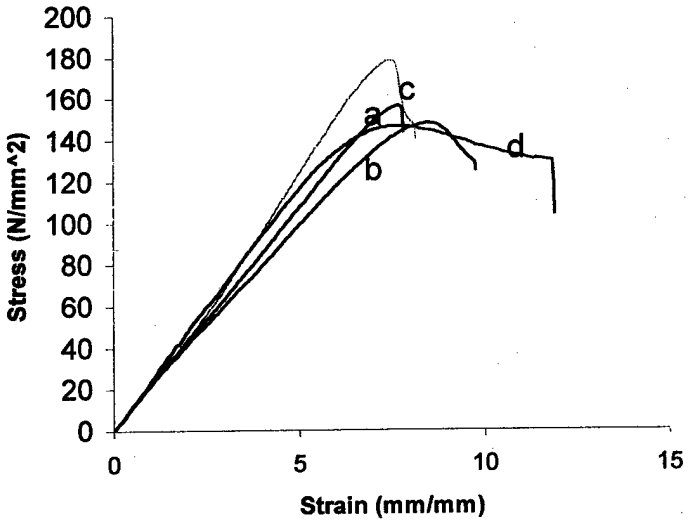

Figure 15 Tensile stress vs. strain plots. (a) Epoxy resin; (b) Rubber dispersed epoxy resin; (c) Clay filled nanocomposite; (d) Rubber dispersed clay nanocomposite.

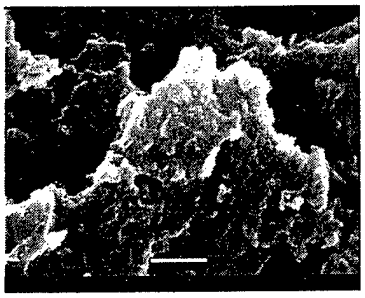

2 (a)

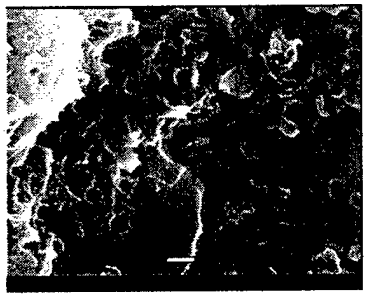

2 (b)

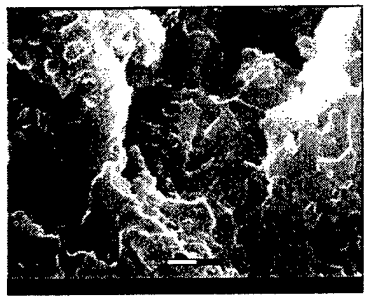

2 (c)

Figure 16 SEM micrographs of tensile fractured surface of (a) Clay filled nanocomposite; (b) Rubber dispersed epoxy; (c) Rubber dispersed clay nanocomposite.

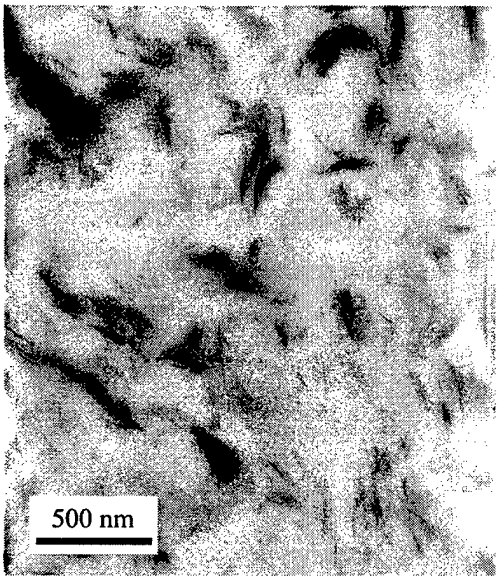

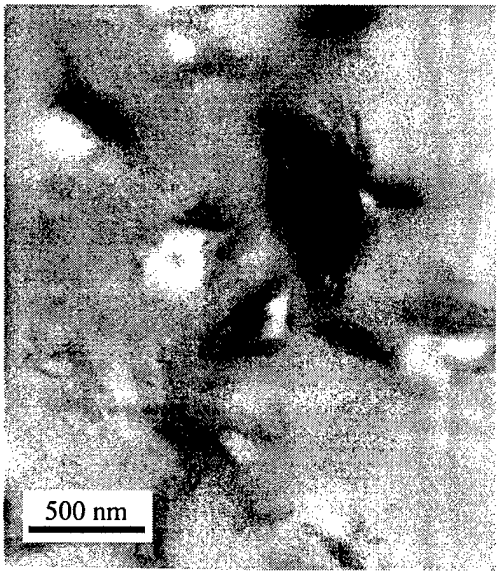

Figure 17 TEM micrographs of (a) Clay filled nanocomposites.; (b) Rubber dispersed clay nanocomposite.